Synthesis and Characterization of Sm-Ho-CeO_2 Compounds Produced by Different Synthesis Methods

[1]Ahmet Hamdi BAKIR and [2]Handan ÖZLÜ TORUN*

[1]*Department of Metallurgical and Materials Engineering, Kahramanmaraş Sütçü İmam University, Kahramanmaraş, Turkey.*

[2]*Department of Energy System Engineering, Kahramanmaras İstiklal University, Kahramanmaras, Turkey.*

handan.ozlutorun@istiklal.edu.tr*

(Received on 13th December 2019, accepted in revised form 23rd November 2020)

Summary-The most important part of a solid oxide fuel cell is the ceramic electrolyte. In this study, cerium oxide (CeO_2) was used as the ceramic electrolyte, and different dopant types were used to increase total conductivity. In this study, the most commonly used Sm, and the less frequently used Ho elements were doped simultaneously. As a result, the effect of dope and different synthesis methods on electrolyte properties was evaluated. Three rates were studied with the total amount of Sm-Ho being 20%. The effect of the dopant types on conductivity with critical radius effect was investigated. These dope types were placed in a CeO_2 crystal lattice by using the sol-gel and hydrothermal methods. After synthesis, the stable phase was obtained at room temperature. X-ray powder diffraction (XRD) was used for phase determination. The thermogravimetry (TG) determined mass change. Scanning electron microscopy (SEM) was used in the analysis of surface morphology. Total conductivity measurements were measured by the four-probe dc method. After synthesis processes, cubic compounds were obtained. The total conductivity values of the cubic phases samples obtained by two different synthesis methods were compared. The highest conductivity was observed in the sol-gel compounds. The highest electrical conductivity $Ce_{0.80}Sm_{0.10}Ho_{0.10}O_2$ system sol- gel; $6.92x10^{-3}(\Omega cm)^{1-}$ at 655 ºC. It was found that the compound obtained as a result of the evaluations could be used ceramic electrolyte application.

Keywords: Ceramic electrolyte, Co-doped, Sol-gel, Hydrothermal, Solid Oxide Fuel Cell.

Introduction

In recent years, solid oxide fuel cells have attracted great attention as an alternative power source due to their high efficiency. However, their use at elevated temperatures raises system costs which, in turn, limit their usage areas. To overcome this problem, electrolyte selection can be used to reduce the working heat of solid oxide fuel cells. Compounds such as ZrO_2, Bi_2O_3, $LaGaO_3$ and CeO_2 are used as ceramic electrolytes [1]. Cerium oxide (CeO2) is frequently studied because these show high oxygen conductivity at low temperatures.

Pure CeO_2 and its compounds are used in various fields such as magnetic materials, photo catalysis, gas sensors, optical materials, fuel cells [2-5]. Pure CeO_2 shows electronic conductivity at high temperatures and a low oxygen pressure. If CeO_2 is used as a ceramic electrolyte, oxygen exhibits ionic conductivity [6]. Impurity doped CeO_2 exhibits ionic conductivity. Different types of doped CeO_2 affect oxygen vacancy concentration and lattice strain [6, 7]. The ionic radius of the dopant cation, dopant amount, synthesis methods, the oxygen ion bond energy and the enthalpy affect the conductivity of the electrolyte [8]. The migration of oxygen ions depends on the amount of impurities and should not exceed 20% [9]. Until now, researches have been conducted to improve the conductivity properties of the electrolytes by using only one type of impurities. The cationic species of bivalent (Ca^{2+}, Mg^{2+}, Ba^{2+}, etc.) and trivalent (Sm^{3+}, Y^{3+}, Er^{3+}, etc.) have been doped into CeO_2, and their properties have been investigated [10-15]. Recent studies have shown that co-doped contributions increase the conductivity at low temperatures compared to single doped [15]. In a study conducted by Ramesh and Raju, It was observed that the conductivity of the binary dopant increased by 11.5%. At the same time, the electronic conductivity of the co-doped ceria electrolyte can be neglected at low temperatures and a high oxygen pressure [16, 17].

There are various synthesis methods for ceramic electrolyte. These methods may affect the microstructure and electrical conductivity of the electrolyte [6, 18]. Conventional methods such as solid-solids, sol-gel, co-precipitation, glycine nitrate, hydrothermal and ultrasounds are commonly used for the synthesis of ceramic electrolytes [18-22].

In the present study, the conductivities of cerium electrolytes synthesized by different methods were investigated and compared. The sol-gel and hydrothermal methods were used in this study. Two different trivalent cations, namely Sm and Ho, which were selected as the dopant type were doped

*To whom all correspondence should be addressed.

simultaneously. Our studies, results of three different ratios were compared. The total dopant amount was determined as 20%. In addition, the effect of different calcination temperatures on the crystal structure was evaluated.

Experimental

The samples in the electrolyte system, $Ce_{0.8}Sm_{0.2-x}Ho_xO_{2-\delta}$ (x= 0.05, 0.1, 0.15), were synthesized by using the sol-gel and hydrothermal methods. In the hydrothermal synthesis processes, cerium(III)nitrate hexahydrate [$Ce(NO_3)_3{\cdot}6H_2O$)] (pure 99,99%, Alfa Aesar), samarium(III)nitrate pentahydrate [$Sm(NO_3)_3{\cdot}6H_2O$)] (pure 99,9%, Arcos organics) and holmium(III)nitrate hexahydrate [($Ho(NO_3)_3{\cdot}6H_2O$)] (pure 99,9%, Arcos organics) were used as the starting materials. Water was used as the solvent in the hydrothermal method. The hydrothermal synthesis was set at 180 ºC for 12 hours. The sample taken from the teflon cap was filtered and washed several times with distilled water. The sample was then dried overnight at room temperature. The samples were grinded with agate mortar and sintered in alumina crucible. Calcination was carried out at 300 ºC and 600 ºC for 12 hours.

In the sol-gel method, the nitrate compounds were dissolved in 30 ml of distilled water, then 5 g of citric acid was added and mixed by using a magnetic stirrer. Ethylene glycol was added to the clear solution. The clear solution was heated on a hot plate at 80-90 ºC. Heating was continued until the color orange appeared in the viscous gel. The gelled sample was kept at 110 °C for 12 h. After firing, the sample turned brown. Then, the sample was ground and calcined at 600, 800 and 1000 °C for 12 hours, respectively.

X-ray diffraction (XRD), (Philips X' Pert Pro, λ = 0.154056 nm, Cu-Kα radiation) was used to characterize the crystal structures and phases of the samples. The total conductivity was measured using the dc four-probe method in the temperature range of 100-800 °C. Pellets with a diameter of 10 mm were prepared from the powder samples with the help of a hydraulic press with pressure around 600 MPa. Before the conductivity measurement, the pellets were sintered at 1300 °C for 10 h. After the sintering and measuring the conductivity, the surface morphology and microstructure of the co-doped CeO_2 was examined by scanning electron microscopy (SEM) (Zeiss EVO 10LS). Thermal behavior was determined from thermo gravimetric (TG)(Perkin Elmer Diamond) analysis at a heating rate of 10 ºC/ min in air and platinum curable from room temperature to 1000 ºC.

Results and Discussion

The XRD patterns of $Ce_{0.8}Sm_{0.2-x}Ho_xO_{2-\delta}$ (x= 0.05, 0.1, 0.15) synthesized at different temperatures and using different methods were recorded and are presented in Figs 1 and 2. The typical cubic fluorite structure was obtained by simultaneously doping Sm and Ho in CeO_2.

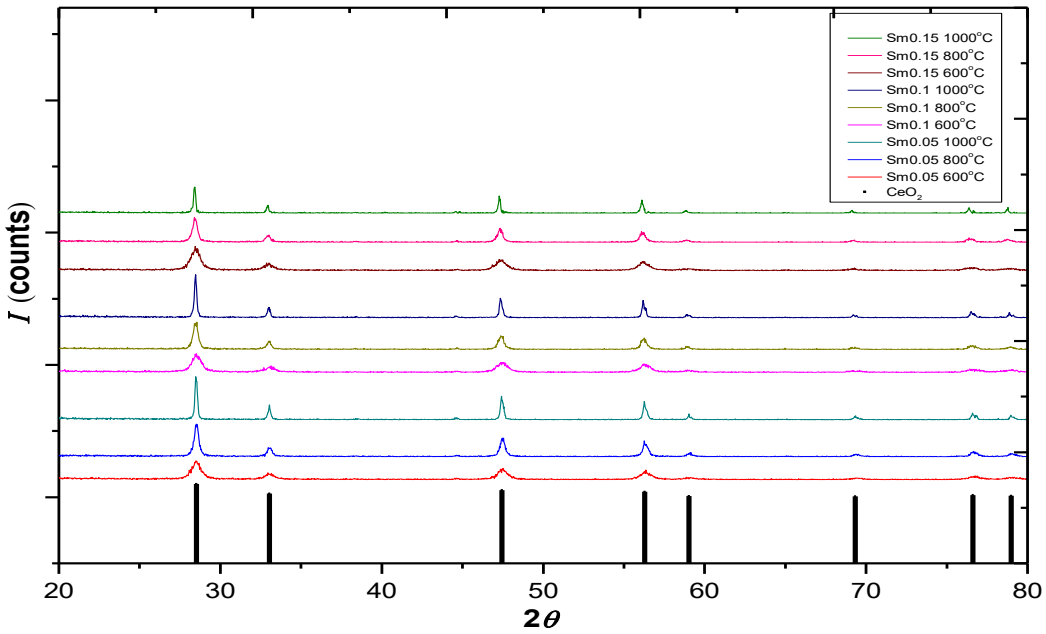

Fig. 1: XRD of the compounds obtained by the sol-gel method based on Sm dope ratio.

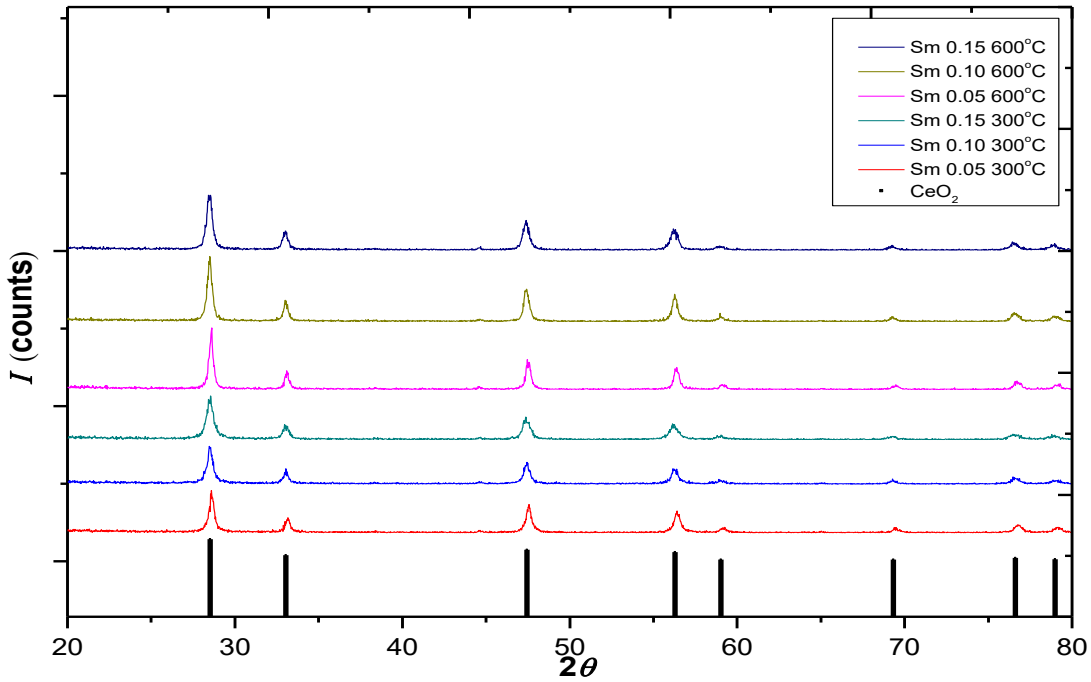

Fig. 2: XRD of the compounds obtained by the hydrothermal method based on Sm dope ratio.

The lattice parameters and crystalline sizes of the samples produced by the hydrothermal method at different calcinations temperatures are given in Table-1. Similarly, in Table-2, the physical characteristics of the powders synthesized by the sol-gel method are given. The CeO_2 unit cell constant was a = 5.407 Å[23]. When tables 1 and 2 are examined, it can be seen that the unit cell parameter increased with the amount of Sm. This change is due to the difference of ionic radii of dope type. The ionic radius values of the dope were Ce^{4+} -0.97 Å, Sm^{3+} -1.079 Å, Ho^{3+} -1.015 Å[24]. The crystal dimensions of the powders were calculated by Debye-Scherer equation (Eq.1-2). It's used Scherrer equation of High Score Plus software;

$$D = \frac{0.89\,\lambda}{\beta\,cos\theta} \quad \beta = \beta_{obs} - \beta_{std} \tag{1}$$

$$\varepsilon = \frac{\beta}{4\tan\theta} \quad \beta = \sqrt{(\beta_{obs}^2 - \beta_{std}^2)} \tag{2}$$

where, D is the crystal size, λ is the CuKα radiation (1.54 A), β is the maximum peak half-length width (FWHM), [theta] is the XRD diffraction pattern obtained from the maximum peak 2 and the [theta] value is the Bragg angle value. 3 peaks with the sharpest diffraction peaks were used in the calculations. The reflection from the (111), (002), (022) plane was used to calculate the average crystallite size.

Table-1: Hydrothermal synthesis XRD results.

Samples	Lattice parameters	Space Group	Volume	Crystalline size
	a (Å)		$(Å)^3$	(nm)
$CeSm_{0.05}Ho_{0.15}$ 300 °C	5.4113	Fm-3m	158.45	30.96
$CeSm_{0.1}Ho_{0.1}$ 300 °C	5.4207	Fm-3m	159.28	28.71
$CeSm_{0.15}Ho_{0.05}$ 300 °C	5.4274	Fm-3m	159.88	21.09
$CeSm_{0.05}Ho_{0.15}$ 600 °C	5.4137	Fm-3m	158.66	34.31
$CeSm_{0.1}Ho_{0.1}$ 600 °C	5.4213	Fm-3m	159.73	30.49
$CeSm_{0.15}Ho_{0.05}$ 600 °C	5.4266	Fm-3m	159.81	25.29

Table-2: Sol-gel synthesis XRD results.

Samples	Lattice parameters a (Å)	Space Group	Volume (Å)^3	Crystalline size (nm)
$CeSm_{0.05}Ho_{0.15}$ 600 ºC	5.416	Fm-3m	158.9	16.35
$CeSm_{0.1}Ho_{0.1}$ 600 ºC	5.421	Fm-3m	159.32	13.2
$CeSm_{0.15}Ho_{0.05}$ 600 ºC	5.428	Fm-3m	159.91	17.2
$CeSm_{0.05}Ho_{0.15}$ 800 ºC	5.4176	Fm-3m	159,0	31.72
$CeSm_{0.1}Ho_{0.1}$ 800 ºC	5.4256	Fm-3m	159.72	26.0
$CeSm_{0.15}Ho_{0.05}$ 800 ºC	5.435	Fm-3m	160,58	26.8
$CeSm_{0.05}Ho_{0.15}$ 1000 ºC	5,420	Fm-3m	159,20	73.45
$CeSm_{0.1}Ho_{0.1}$ 1000 ºC	5,428	Fm-3m	159,95	64,9
$CeSm_{0.15}Ho_{0.05}$ 1000 ºC	5,434	Fm-3m	160,42	46.22

As shown in Table-1 and 2, the increase in the calcination temperature of the powder ceramic electrolytes synthesized by both the hydrothermal and sol-gel methods partially caused crystalline size growth. As a result of the calculations, it can be seen that there is a linear relationship between the increase in crystal size and temperature. As the temperature increased, the width of the peaks became narrower. This can be explained by increasing the diffusion rate of the particles in the temperature. There cannot always be a linear relationship between the crystal size and the unit cell parameter. It depends on the magnetic properties of the compound and the stresses that occur within the structure [25, 26].

When the thermal analysis graphs are examined (Fig 3), it can be seen that the mass loss after the gel form was approximately 60-70%. For this reason, nitrate, ethyl glycol, molecular water, and the citric acid were removed. The boiling temperature of citric acid is approximately 450-500 ºC. After 600 ºC, there was almost no mass loss. However, when the curves in Fig 3 taken from the heat treated sample are examined, it is seen that the mass loss in the TG curve was quite low. In the hydrothermal method, the mass loss was between 4-6%. After the samples were taken from the autoclave, filtration and washing were performed. Water was available in the structure after washing since the drying cannot be ultimately achieved.

The effect of the synthesis method on the microstructure was evaluated by the SEM image. The ceramic samples with the whole cubic crystal lattice were sintered at 1300 ºC and for 10 hours after being pelletized under 500 MPa pressure. In the sintering process, the single temperature and time were used. Temperature and time-related morphological studies were excluded. Sectional images were not examined since the press samples were compressed by pressing.

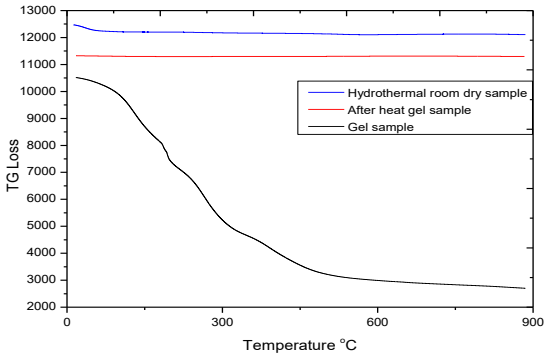

Fig. 3: Mass change graph of sol-gel synthesis and hydrothermal synthesis.

When the images are examined, it can be seen that there were apparent differences in the particle structure due to the method used. According to the morphological results of the sol-gel method, the particle distribution was homogeneous, and the particle sizes were around 320 nm (Fig. 4). Pellets sample had little porosity in the structure. The particle size is one of the essential factors affecting conductivity. As the particle size decreases, the conductivity value increases [27]. This porosity and grain distribution encountered in the left gel method allowed the oxygen-ionic conductivity as well as the electronic conductivity in conductivity.

In the samples obtained by the hydrothermal method, according to the SEM surface images, the grain size was approximately 1-1.2 microns (Fig 4). This grain size is due to the combination of a large number of particles. There was almost no porous structure and the grain size was not uniform. The stoichiometry of all samples phase was verified by the EDS microanalysis. According to the results of EDS, the crystal structure consisted of the Ce-Sm-Ho-O elements (Table- 3 and 4). The proportions of the final compounds were very close to the initial stoichiometry.

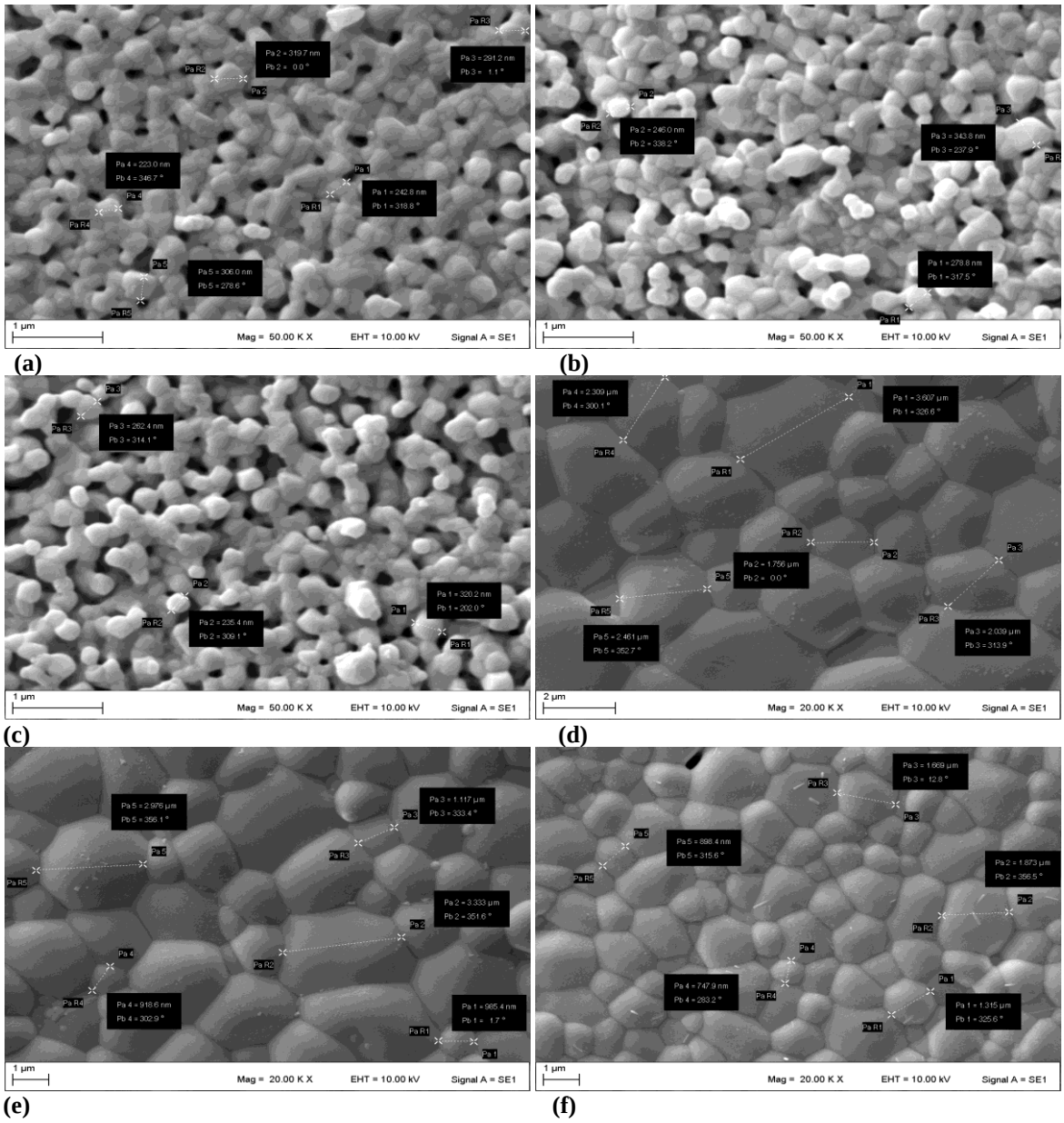

Fig. 4: SEM images for the A, B, C sol-gel samples and D,E,F hydrothermal samples**.**

Table-3: Hydrothermal synthesis EDS results.

Element	ht1 C norm. wt %	ht2 C norm. wt %	ht3 C norm. wt %
Cerium	**76.94**	**78.22**	**76.26**
Oxygen	**2.90**	**2.33**	**4.51**
Samarium	**15.54**	**10.30**	**3.92**
Holmium	**4.62**	**9.16**	**15.31**
Total	**100 %**	**100 %**	**100 %**

Table-4: Sol-gel synthesis EDS results.

Element	s1 C norm. wt %	s2 C norm. wt %	s3 C norm. wt %
Cerium	**73.53**	**73.89**	**73.49**
Oxygen	**6.32**	**5.62**	**5.41**
Samarium	**14.70**	**9.81**	**4.36**
Holmium	**5.45**	**10.68**	**16.75**
Total	**100 %**	**100 %**	**100 %**

The conductivity of the co-doped CeO_2 was measured by the dc four-probe method. The conductivity of the powder samples with cubic structure was pelleted with a diameter of 10 mm and at 500MPa before the measurements. Pellet sample was sintered at 1300 ^oC for 10 hours. Platinum wire with the best conductivity and resistant to high temperatures was used for the analyses. The distances between the wires were equal. The circular samples were placed on a ceramic sample holder while conducting the conductivity measurements. The temperature during the measurements was increased up to 800 ^oC starting from room temperature. The measurement range was increased by 50 ^oC up to 400

ºC. After 400 ºC, it was increased by 20 ºC. The samples were waited 10 minutes for stability at each temperature. The average of 10 values was taken for each temperature. The circular structure was entered in the geometric structure factor when evaluating the measurements.

CeO_2 is nonconductive at low temperatures. CeO_2 can be become conductive by doping and the oxygen-ion conductivity value σ depends strongly on the temperature. The oxygen-ion conductivity value in this study was 4.4181×10^{-4} scm^{-1} at 530 °C [28]. The conductivity of CeO_2 was increased by doping. In this study, it was determined that the Sm-Ho contribution increased conductivity. When the graphs were examined in both methods, a linear increase in conductivity values was observed depending on the temperature (Fig 5 and 6). Oxygen vacancies occurred with the addition of Sm and Ho. This can explained for trivalent dopant type by the Kroger V Ving equation. [29, 30];

$$M_2O_3 + 2Ce_{Cex} + 4O_{Ox} \rightarrow 2M_{Ce2} + V_o{}^{\cdot\cdot} + 3O_{Ox} + 2CeO_2$$

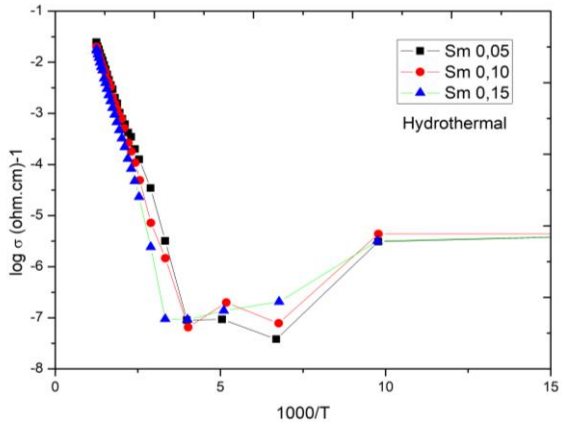

Fig. 5: Total conductivity change graph of the compounds synthesized by the hydrothermal method.

The increase in conductivity value is based on the doped type selection. According to Omer et al., critical dopant ionic radius is important [23]. 1.0252 Å is a critical radius value. Sm increases conductivity and Ho decreases. The ionic radius values of the dope are Sm^{3+}- 1.079 Å, Ho^{3+} -1.015 Å. The average radius of dope types is 1.047 Å and higher than the critical radius value. In both methods, the conductivity value decreases depending on the amount of holmium. Holmium cations reduce oxygen diffusion rate and decrease conductivity. Furthermore, the holmium cation radius is below the crotch radius.

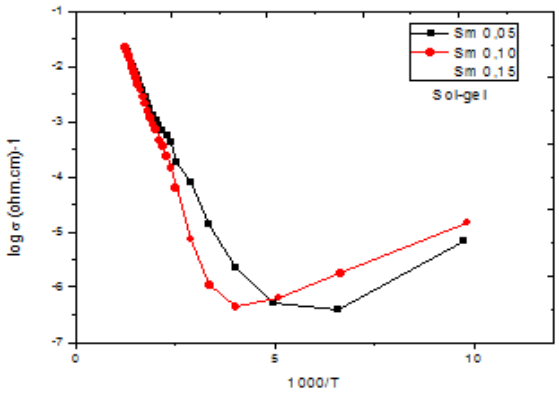

Fig. 6: Total conductivity change graph of the compounds synthesized by the sol-gel method.

When conductivity graphs were compared (Fig 7), the conductivity value of the samples synthesized by the sol-gel method was higher. The reason for this is that the intergranular pores also contributed to electronic conductivity, increasing the total conductivity values. Although the conductivity of hydrothermal synthesis at 550 ºC seems better, the conductivity of sol-gel synthesis compounds improved as the temperature increased (650 ºC). This is also related to the grain and crystal size.

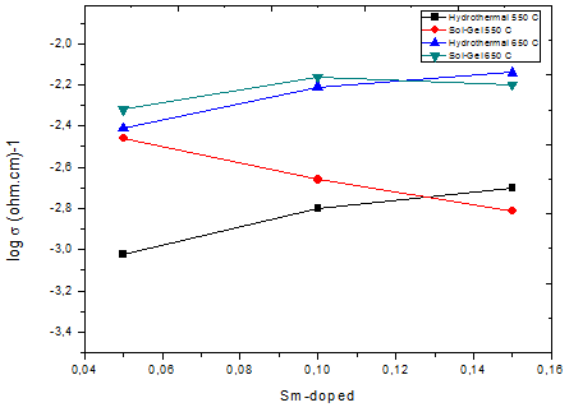

Fig. 7: Method and temperature comparative total conductivity graph.

Conclusion

In this study, it was investigated how Sm and Ho changed pure CeO_2 conductivity by doping together. Using two different synthesis methods, the sol-gel and hydrothermal methods, compounds were synthesized in the cubic crystal structure in the same stoichiometric ratios. According to the results of the thermal analysis, it was determined that there was no

mass loss at 750 ºC and above, and the corrupt species were completely removed from the environment. When the microstructural properties were compared, the particles obtained by the sol-gel synthesis were found to be of lower size. According to the total conductivity data, Ho had a negative contribution. The highest conductivity was observed in the sol-gel compounds.

Acknowledgment

The authors would like to thank the Scientific Research Projects unit of Kahramanmaraş Sütçü İmam University for supporting this study (Project Number: 2018/2-26).

References

1. J.W. Fergus, Electrolytes for solid oxide fuel cells. *J. Power Sources*, **162,** 30 (2006).
2. C. Zhang, F. Meng, L. Wang Controlled synthesis and magnetic properties of bowknot-like CeO_2 microstructures by a CTAB-assisted hydrothermal method. *Materials Letters*, **119**, 1 (2014).
3. Z. Fan, F. Meng, J. Gong, H. Li, Y. Hu, D. Liu, Enhanced photocatalytic activity of hierarchical flower-like CeO_2/TiO_2 heterostructures. *Materials Letters*, **175**, 36 (2016).
4. L. Wang, F. Meng, Oxygen vacancy and Ce^{3+} ion dependent magnetism of monocrystal CeO_2 nanopoles synthesized by a facile hydrothermal method. *Materials Research Bulletin*, **48**, 3492 (2013).
5. F. Meng, L. Wang, J. Cui, Controllable synthesis and optical properties of nano-CeO_2 via a facile hydrothermal route. *J.Alloys and Com.*, **556**, 102 (2013).
6. N. Mahato, B. **A**mitava, G. Alka, O. Shobit, B. Kantesh. Progress in materials science progress in material selection for solid oxide fuel cell technology: a review. *Prog.Mater Sci*.,**72**, 141 (2015).
7. S.V. Chavan, A.K .Tyagi, Phase relations and lattice thermal expansion studies in the $Ce_{0.50}RE_{0.50}O_{1.75}$ (RE= rare-earths). *Materials Sci. and Eng.: A*, **404**, 57 (2005).
8. K. C. Anjaneya, G.P. Nayaka, J. Manjann, G. Govindaraj, K.N Ganesha, Preparation and characterization of $Ce_{1-x}Gd_xO_{2-\delta}$ (x= 0.1–0.3) as solid electrolyte for intermediate temperature SOFC. *J.Alloys and Compounds*, **578**, 53 (2013).
9. C.C. Chou, C.F. Huang, T.H .Yeh, Investigation of ionic conductivities of CeO2-based electrolytes with controlled oxygen vacancies. *Ceramics International*, **39**, 627 (2013).
10. N. Chaubey, B. N. Wani, S. R. Bharadwaj, M.C. Chattopadhyaya Physicochemical properties of rare earth doped ceria $Ce_{0.9}Ln_{0.1}O_{1.95}$ (Ln= Nd, Sm, Gd) as an electrolyte material for IT-SOFC/SOEC. *Solid State Sci*., **20**, 135 (2013).
11. K .Tanwar, N. Jaiswal, D. Kumar, O. Parkash, Synthesis & characterization of Dy and Ca Co-doped ceria based solid electrolytes for IT-SOFCs. *J. Alloys and Compounds*, **684**, 683 (2016).
12. J. Yang, B. Ji, J. Si, Q. Zhang, Q. Yin, J. Xie, C.Tian. Synthesis and properties of ceria based electrolyte for IT-SOFCs. *Int. J. Hydrogen Energy*, **41**, 15979 (2016).
13. J .Van Herle, D. Seneviratne, A. J. McEvoy. Lanthanide co-doping of solid electrolytes: AC conductivity behaviour. *J. European Ceramic Soc.*, **19**, 837 (1999).
14. Y. H.Ahiro, K. Eguchi, H. Arai, Electrical properties and microstructure in the system ceria-alkaline earth oxide. *J.Materials Sci.*, **23**, 1036 (1988).
15. R. Raza, X. Wang, Y. Ma, B. Zhu, Study on calcium and samarium co-doped ceria based nanocomposite electrolytes. *J. Power Sources*, **195**, 6491 (2010).
16. S. K. Tadokoro, E.N.S. Muccillo Effect of Y and Dy co-doping on electrical conductivity of ceria ceramics. *J. European Ceramic Soc.*, **27**, 4261 (2007).
17. S. Ramesh, K. J. Raju Preparation and characterization of $Ce_{1-x}(Gd_{0.5}Pr_{0.5})_xO_2$ electrolyte for IT-SOFCs. *Int.J. of Hydrogen Energy*, **37**, 10311 (2012).
18. G. Kim, N. Lee, K.B. Kim, B.K. Kim, H. Chang, S.J. Song, J.Y. Park Various synthesis methods of aliovalent-doped ceria and their electrical properties for intermediate temperature solid oxide electrolytes. *Int. J. Hydrogen Energy*, **38**, 1571 (2013).
19. H. Okkay, M Bayramoğlu, M.F. Öksüzömer Ultrasound assisted synthesis of Gd and Nd doped ceria electrolyte for solid oxide fuel cells. *Ceramics International*, **39**, 5219 (2013).
20. H. O. Torun, S. Çakar, Thermal characterization of Er-doped and Er–Gd co-doped ceria-based electrolyte materials for SOFC. *J.Thermal Analysis and Calorimetry*, **133**, 1233 (2018).
21. O. Mendiuk, M. Nawrocki, L. Kepinski, The synthesis of Ce1− xLnxO2− y (Ln= Pr, Sm, Gd, Tb) nanocubes by hydrothermal methods. *Ceramics International*, **42**, 1998 (2016).
22. F. Meng, J. Gong, Z. Fan, H. Li, J. Yuan, Hydrothermal synthesis and mechanism of triangular prism-like monocrystalline CeO_2 nanotubes via a facile template-free

hydrothermal route. *Ceramics International*, **42**, 4700 (2016).

23. S. Omar, E. D. Wachsman, J.L. Jones, J.C. Nino Crystal structure–ionic conductivity relationships in doped ceria systems. *J. American Ceramic Society*, **92**, 2674 (2009).
24. R.D. Shannon, CD Prewitt. Effective ionic radii in oxide and fluorides. *Acta Crystallog*. **25**,925–46(1969).
25. D. Kumar, M. Singh, A. K. Singh, Crystallite size effect on lattice strain and crystal structure of $Ba_1/4Sr_3/4MnO_3$ layered perovskite manganite. In *AIP Conference Proceedings* **1953**, 030185 (2018).
26. U.Shankar, , A. K. Singh, Origin of suppression of charge ordering transition in nanocrystalline Ln0. 5Ca0. 5MnO3 (Ln= La, Nd, Pr) ceramics. *The J. of Phy. Chem*., **119**(51), 28620-28630(2015).
27. X. D. Zhou, W. Huebner, I. Kosacki, H.U. Anderson Microstructure and grain-boundary effect on electrical properties of gadolinium-doped ceria. *J. American Ceramic Soc*., **85**, 1757 (2002).
28. H. Jin, N. Wang, L. Xu, S.Hou, Synthesis and conductivity of cerium oxide nanoparticles. *Materials Letters*, **64**, 1254 (2010).
29. M. N. Rahaman *Sintering of ceramics*. CRC press(2007) .
30. K. Schwarz Materials design of solid electrolytes. *Proc. of the National Academy of Sci.*, **103**, 3497 (2006).